ARCHIVES OF ELECTRICAL ENGINEERING VOL. X(Y), pp. 1-23 (2027)

This paper has been accepted for publication in the AEE journal. This is the version, which has not been fully edited and content may change prior to final publication.
Citation information: DOI 10.24425/aee.2027.8064

Single-period unit commitment improvement based on optimal power flow with renewable energy sources using a hybrid of whale optimization algorithm and differential evolution

ZAİNAB ALİ HABEEB*, LAYTH TAWFEEQ ALBAHRANİ

Mustansiriyah University, College of Engineering, Electrical Engineering Department
Baghdad, Iraq
*e-mail: {*zainab1985/Layth1973a}@uomustansiriyah.edu.iq*

Received: 02.08.2026, revised: ……..)

Early Access

Abstract: This article proposes a single-period unit commitment enhancement for specified system load to minimize two separate objective functions of economic operations: fuel cost of thermal power generation units and active power losses of transmission based on Optimal Power Flow (OPF) using a hybrid optimization technique of the Whale Optimization Algorithm and Differential Evolution (WOA-DE). The proposed algorithm included the renewable energy resource of wind turbines, considering the wind speed uncertainty with a Weibull distribution model to estimate wind power output. The wind turbines have been installed based on optimal locations using the WOA-DE technique. The control variables of optimal power flow were initially optimized to minimize two separate objective functions of fuel cost and active power losses for each one. These control variables are the generator active power except the slack, the generator voltage magnitude, the transformer tap setting, the shunt compensation reactive power and the locations of renewable energy resources. OPF output was accessed during each progressive unit shutdown. Integrating renewable energy improves the flexibility of the unit commitment schedule by decreasing the number of thermal generating units taken offline without compromising system feasibility. The proposed WOA-DE-based framework can support more economical and reliable operation of the power system by improving unit commitment decisions, increasing the installation of the renewable energy sources, and enabling satisfying the operational constraints of the power system. The novelty of the proposed framework lies in integrating Weibull-based wind recourse characterization, optimal wind turbine placement, single-period unit commitment, and optimal power flow within a hybrid WOA-DE optimization framework to assess power system operation before and after renewable energy integration. The proposed technique is implemented on the IEEE 30 bus test system.

Keywords: Differential Evolution (DE), Optimal Power Flow (OPF), Renewable Energy Source (RES), Unit Commitment (UC), Whale Optimization Algorithm (WOA)

This paper has been accepted for publication in the AEE journal. This is the version, which has not been fully edited and content may change prior to final publication.
Citation information: DOI 10.24425/aee.2027.8064

1. Introduction

Modern power systems require coordinated management of generation scheduling, network operating conditions, and load requirements to be economically viable and run efficiently. The OPF is typically used to determine the optimum steady-state operating point by satisfying both the AC load-flow equations and the defined system operating limits. Most standard OPF studies focus solely on minimizing the fuel costs and the active power losses. However, the addition of Renewable Energy Sources (RESs), such as wind generation, affects the net power injections into the network and may change the system's optimum operating point.

Several studies on OPF, renewable energy integration, and Unit Commitment (UC) have been conducted extensively. Data from studies conducted by Duman and others have demonstrated the effect of the RES on the operating costs and system performance of both the IEEE 118 and IEEE 30-bus systems by solving the AC OPF problem for wind, thermal, solar, and tidal generation. While the Duman *et al*. studies investigated the effects of integrating RESs on system operating costs and overall performance [1]. Alghamdi conducted an OPF study on the IEEE 30 bus system, combining the GWOPSO algorithm with hybrid metaheuristic techniques and demonstrating improvements in the solution of non-linear OPF problems [2]. Saleh investigated UC, economic dispatch, and OPF (with and without wind generation) for the IEEE 30 bus test system and showed that integrating wind generation affects both overall operating costs and the scheduling of generation resources [3]. Siregar *et al*. in a separate study, proposed a unit commitment framework using OPF to manage renewable-based power systems at various load levels [4].

Recent studies have been conducted on hybrid optimization, renewable uncertainty, and generation scheduling under network constraints. Riaz *et al*. introduced a hybrid particle swarm-Grey Wolf optimizer for solving the optimal power flow problem in IEEE 30-bus systems incorporating wind and solar energy and taking into account generation costs, emissions, and losses in active power [5]. Li *et al*. proposed a two-stage robust unit commitment method with linearized AC power flow constraints aimed at addressing uncertainty of renewable energy [6]. Mena *et al*. introduced a multi-objective two-stage stochastic UC model for systems with wind energy integration while considering costs of operation, emissions of CO_2, and curtailment of wind energy produced [7]. Gholami Trojani *et al*. proposed a stochastic UC formulation which includes renewable generation, energy storage systems, electric vehicles, and flux loads [8]. Niu *et al*. recently introduced a unit commitment model taking into account the integration of renewable energy sources and electric vehicles, using a Binary Covariance Matrix Adaptation Evolution Strategy (BCMAES) that has proved effective in minimizing costs and emissions even under variability conditions [9].

Several recent works have investigated the integration of unit commitment with optimal power flow and renewable sources, using different optimization techniques and solution methods. Some studies treated UC and OPF as distinct optimization problems, while other methods relied on various metaheuristic algorithms, with the performance of the search being affected by the balance between the two processes. The novelty of the present research consists

Early Access

This paper has been accepted for publication in the AEE journal. This is the version, which has not been fully edited and content may change prior to final publication.
Citation information: DOI 10.24425/aee.2027.8064

of creating an OPF-based unit commitment model for optimizing the integration of renewable sources into the system, applying a hybrid WOA-DE solution method. The original aspect of this research lies in the combining the WOA technique with the mutation, crossover, and refinement procedures of the DE technique, allowing the researchers to level the imbalance between exploration and exploitation compared to using either method alone. Also, the OPF stage helps evaluate the unit commitment decisions according to the constraints related to the operating of the network and the influence of the renewable source generation. Overall, the employment of the model enables the creation of the method that is able to develop profitable and realizable schedules for power generation in renewable sources-oriented power systems.

This article proposes a sequential OPF unit commitment enhancement framework that combines the Whale Optimization Algorithm and Differential Evolution (WOA-DE) to find the optimal location of the RES and improve the efficiency of unit commitment. The adopted methodology has been presented for the IEEE 30-bus system. The first stage of the research will determine OPF solutions without Renewable Energy Sources (RESs) for two independent objectives: the minimum fuel cost and the minimum active power loss. The next stage will be to incorporate renewable energy sources into the unit commitment problem and to include their locations in the control variable vector to determine the optimal location for each of the two objectives. Unit commitment is performed as the final stage of the OPF process. The optimal operating point is used to assess whether thermal generators are either online (operating) or offline (not operating).

To further highlight the differences between the current work and related OPF-assisted UC studies, Table 1 summarizes the key characteristics of the reviewed studies regarding the formulation of UC, integration of renewable energy, optimization approach, objectives, and type of system under examination.

Early Access

Table 1. Comparison of the proposed approach with related UC and OPF-assisted UC studies

Study	Objectives	Test system	Main distinguishing feature
[3], 2022	cost	IEEE 30 bus	UC, ED, and OPF cooperation before and after adding RES (wind farm) using optimization technique of power system simulator for engineering PSS®E.
[4], 2025	cost and losses	IEEE 30 bus	UC and OPF evaluated under multiple load levels with RES (PV) using the optimization technique of Mixed Integer Nonlinear Programming (MINLP) and PSO-assisted OPF.
[6], 2023	cost	Modified NERL-118	UC, ED, and OPF considering RES (wind farm and PV) using the optimization technique of a robust optimization method
Proposed study	Cost and losses	IEEE 30 bus	UC, ED, and OPF cooperation before and after adding RES (wind farm) using the optimization technique of the hybrid algorithm WOA-DE

This paper has been accepted for publication in the AEE journal. This is the version, which has not been fully edited and content may change prior to final publication.
Citation information: DOI 10.24425/aee.2027.8064

The present work deals with a unit commitment problem in one time period given a fixed load and incorporates an optimization approach to unit commitment assisted by optimal power flow, wind energy resource characterization based on the Weibull distribution, optimal wind farm placement, and comparison of the achievements in renewable energy integration.

The contribution of this study is the development of an integrated framework that combines OPF for optimal placement of the RES according to the objective and, thereafter, an enhancement of the UC based on these RES and OPF solutions.

2. Mathematical formulation

2.1. Load flow equations

The equations for active and reactive power balance for bus i in a system with N buses are given by [10]:

$$P_i = PG_i - PL_i = V_i \sum_{j=1}^{N} V_j \ (G_{ij}\cos\theta_{ij} + B_{ij}\sin\theta_{ij}), \tag{1}$$

$$Q_i = QG_i - QL_i = V_i \sum_{j=1}^{N} V_j \ (G_{ij}\cos\theta_{ij} - B_{ij}\sin\theta_{ij}), \tag{2}$$

where P_i and Q_i denote the net active and reactive power injections at bus i, respectively, and PG_i and QG_i denote the active and reactive power generation, respectively, and PL_i and QL_i are the active and reactive load demands at bus i, respectively, and V_i and V_j are the voltages at buses i and j, respectively, G_{ij} and B_{ij} are the conductance and susceptance of the line respectively, $\theta_{ij} = \delta_i - \delta_j$ is the angle difference between the two voltages at bus i and bus j respectively.

Early Access

2.2. Variables in OPF

Two types of variables in OPF need to be satisfied. The first are the control variables, which can be adjusted from their limits based on the optimization algorithm. The second is the state variables obtained from the power-flow study.

2.2.1. Control variables

The control variables in this article consist of five types of control variables, which are the active power of generators except the slack PG, the voltage magnitudes of the generators VG, transformer tap ratios T, shunt compensation QC, and the locations of renewable sources L^{RES}. The control vector X is given in Eq. (3) [11, 12].

$$X = [PG, VG, T, QC, L^{\mathrm{RES}}], \tag{3}$$

where each control variable has been adjusted using the optimization technique according to its maximum and minimum limits.

This paper has been accepted for publication in the AEE journal. This is the version, which has not been fully edited and content may change prior to final publication.
Citation information: DOI 10.24425/aee.2027.8064

2.2.2. State variables

State variables are dependent quantities found by the AC power-flow solution after each control vector has been applied. They consist of slack generators, active power PG_{slack}, generator reactive powers QG, and voltage magnitudes of load buses VL [11].

$$Y = [PG_{\text{slack}}, QG, VL]. \tag{4}$$

Each state variable will be checked and satisfied according to its condition of maximum and minimum limits. Thus, control variables are optimized directly, whereas state variables are computed from the AC load flow and checked against their allowable limits.

2.3. Objective functions

Two individual OPF objectives were optimized separately. Each objective function has its corresponding optimal control variables, load-flow results, and the optimal RES location. These two objective functions are the fuel cost and the active power losses.

2.3.1. Minimization of fuel cost

The fuel cost of thermal generation units has been calculated according to Eq. (5).

$$\text{Fuel Cost} = \sum_{i=1}^{NG} a_i + b_i PG_i + c_i PG_i^2 \ \$/h, \tag{5}$$

where *NG* refers to the total number of power-generating stations, *i* represents the index of the power-generating station, PG_i refers to the active power output of the generating station *i*, MW, a_i, b_i, and c_i refer to the fuel cost coefficients of the generating station *i*. In this context, a_i means the constant or fixed fuel cost coefficient, b_i is the linear fuel cost coefficient, and c_i refers to the quadratic fuel cost coefficient. Note that the quadratic term $c_i PG_i^2$ presents the nonlinear increase in fuel cost of the generating units as the output power increases. [13]

Early Access

2.3.2. Minimization of active power loss

Active power losses of transmission lines have been calculated according to Eq. (6).

$$P \text{ losses} = \sum TL\ G_{ij}\ (|V_i|^2 + |V_j|^2 - 2|V_i V_j\ |\cos\delta_{ij}, \tag{6}$$

where *P* losses show the overall transmission network electrical power loss in MW; TL indicates the collection of lines in the power system, G_{ij} symbolizes the conductance related to the line transmitting power between buses *i* and *j*; V_i and V_j represent voltages at buses *i* and *j*, respectively, in p.u. units; δ_{ij} shows the difference of voltage angle between bus *i* and bus *j*. [14]

3. Renewable energy modeling and optimal placement

The use of renewable energy sources (wind farms) is included in the OPF model as controllable power injections. The optimal location of their installation is obtained with the proposed optimization algorithm by assessing all potential bus candidates and selecting the

This paper has been accepted for publication in the AEE journal. This is the version, which has not been fully edited and content may change prior to final publication.
Citation information: DOI 10.24425/aee.2027.8064

location that provides maximum performance of the objective function under the operational constraints of the network.

3.1. Renewable power injection model

Renewable energy sources are treated as active power injections at specific buses in a power system. The net load of a bus that receives renewable generation will be adjusted as follows [15]:

$$PD_{\text{net}} = PD_i - P_{\text{RES}i}, \tag{7}$$

where PD_{net} is the net demand, PD_i is the total demand, and $P_{\text{RES}i}$ is the power generation based on renewable energy sources.

The overall active power balance for the power system can be expressed as [16]:

$$\sum_{i=1}^{NG} PG_i + \sum_{j=1}^{N_{\text{RES}}} P_{\text{RES}j} = \sum_{k=1}^{N_B} PD_k + P_{\text{loss}}, \tag{8}$$

where PG_i is the active output power of the conventional generation facility number i; $P_{\text{RES}j}$ is the output of renewable energy facility number j, PD_k is the amount of active electricity consumed at bus k; P_{loss} is the transmission lines active power loss; NG is the number of active conventional generation facilities; N_{RES} is the number of active renewable energy sources connected to energy system; and N_B is the load bus number in the network.

From this equation, the total active power produced by conventional units and the RES must be equal to the total system load demand and active losses through the transmission system.

3.2. Wind power model

Wind speed variability has been represented based on the Weibull probability density function $f(v)$ [17]:

$$f(v) = \frac{k}{c}\left(\frac{v}{c}\right)^{k-1} e^{-\left(\frac{v}{c}\right)^{k}}, \quad v \geq 0, \tag{9}$$

where: v is the wind speed; k is the shape parameter; c is the scale parameter. The corresponding available wind power output has been calculated using the adopted cubic turbine power curve [18]:

$$Pw(v) = \begin{cases} 0 & v < v_{\text{in}} \\ Pr\left(\frac{v^3 - {v_{\text{in}}}^3}{{v_r}^3 - {v_{\text{in}}}^3}\right) & v_{\text{in}} \leq v < v_r \\ Pr & v_r \leq v < v_{\text{out}} \\ o & v \geq v_{\text{out}} \end{cases}, \tag{10}$$

where Pw is wind turbine power generation v_{in} is cut-in speed, v_r is the rated wind speed, v_{out} is cut-out speed. The calculation of wind power generation was based on a simulation of the wind speed for each wind farm using the inverse transform sampling from the Weibull distribution. The resulting wind speed values were converted into available wind power generation using the adopted cubic power curve of the turbine [19]. The fluctuation of wind speed has been statistically characterized by a two-parameter Weibull distribution so as to

Early Access

This paper has been accepted for publication in the AEE journal. This is the version, which has not been fully edited and content may change prior to final publication.
Citation information: DOI 10.24425/aee.2027.8064

calculate the representative operating points for the generation of wind energy. The respective wind power values have been used as constant fixed renewable injections for the OPF and commitment studies. Thus, the present formulation has the nature of a deterministic operating point-based technique as opposed to being a stochastic or scenario-based method.

3.3. Objective-specific RES placement

Each objective for OPF will have its own independently chosen location for the RES, which can include a generator bus or PQ bus. Each candidate bus is then evaluated using the OPF with the WOA-DE, and the one that yields the best objective is accepted as the selected candidate.

4. Hybrid WOA-DE optimization algorithm

The design of the hybrid WOA-DE algorithm incorporates a search capability derived from the Whale Optimization Algorithm (WOA), using the differential evolution refinement process to improve exploration by leveraging the evolutionary ability of Differential Evolution (DE) over time. The hybrid WOA-DE algorithm, implemented within the OPF solutions, was utilized as the consumer-side of electrical energy used to generate solutions to four different OPF objectives: fuel cost minimization and active power loss minimization. In this case, the algorithm will try to find the optimal variables for the operation, together with the best location of the renewable sources, for a given OPF objective [20].

Early Access

4.1. WOA position update

WOA simulates the humpback whale's hunting method; thus, each candidate solution represents an operating point of the electrical system. In this case, each candidate solution would consist of multiple candidate variables, such as voltages of generators, tap transformer positions, shunt compensation, generator active power, and the location of the renewable sources. WOA guides the candidate solutions to word the current best solution using encircling and spiral-search mechanisms. WOA uses an exploratory phase and an exploitative phase to permit all of the candidates in the population to explore multiple locations in the solution space and reduce the population by concentrating the search in smaller regions of the best OPF solutions [21], [22]. The declination is defined by the following equations:

$$a_{\mathrm{woa}} = 2 - 2 \times (t-1)/(T-1), \tag{11}$$

$$D = |C \times X^*(t) - X(t)|, \tag{12}$$

$$X(t+1) = X^*(t) - A \times D, \tag{13}$$

$$A = 2 \times a_{\mathrm{woa}} \times r_1 - a_{\mathrm{woa}}, \tag{14}$$

$$C = 2 \times r_2, \tag{15}$$

This paper has been accepted for publication in the AEE journal. This is the version, which has not been fully edited and content may change prior to final publication.
Citation information: DOI 10.24425/aee.2027.8064

where *t* is the repetitions number, *T* is the of repetitions maximum number, and *C* is a vector that is used to determine how much the existing best solution will have over the encircling process. At *t* + 1, the new candidate *X* has been modified from its previous candidate by an adjustment of *D* times the constant *A*. r_1 and r_2 are random variables, from 0 to 2. The objective is to produce new feasible candidates, *X**, that have lower objective values than their original candidates, *X*.

4.2. DE mutation and crossover

DE is used in combination with the other evolutionary operator (WOA) to foster diversity among all candidates (WOA candidates) and to avoid premature convergence. To form a mutated candidate, the DE operator creates a mutant candidate vector *V* by adding the difference of two randomly chosen mutation candidates, and then uses this vector as the basis for constructing *U*, which will be evaluated against the OPF feasibility requirements. Any vector U that yields better results will be accepted as a new candidate until all candidates are removed from consideration and replaced with newly created candidates [23], as shown in (16) and (17).

$$V_i = X_{r1} + F \times (X_{r2} - X_{r3}), \tag{16}$$

$$U_{ij} = \begin{cases} V_{ij} & if\ j \le CR \\ X_{ij} & \text{otherwise} \end{cases}. \tag{17}$$

If the objective value of the newly created *U* is less than that of the previous candidate, then the

The new *U* is accepted as the new candidate.

4.3. Proposed hybrid flow

1. Set the initial state for population/algorithm parameters.
2. Compute the fitness value for each candidate solution.
3. Choose the current best candidate solution *X**.
4. Update all candidate solutions using equations for WOA.
5. Create mutant vectors by type of DE mutation.
6. Create trial vectors by type of DE crossover using mutated vectors as input.
7. Use selection on the original verse trial solution to keep the best solution.
8. Update the best possible solution thus far.
9. Repeat the loop until total iterations have exceeded the maximum of allowable iterations.

5. Proposed RES-UC-OPF methodology

5.1. Step 1: Unit commitment-based OPF without RES

In step 1, the OPF for the IEEE 30 bus system is solved for each of the two objectives, fuel cost and losses, using WOA-DE with no RES included to solve the problem of UC.

Early Access

This paper has been accepted for publication in the AEE journal. This is the version, which has not been fully edited and content may change prior to final publication.
Citation information: DOI 10.24425/aee.2027.8064

The OPF approach presented here is a preliminary simplified assessment. The main components have been covered, including the main bus, load generator, voltage and transformer tap settings, and shunt compensation schemes, but the transmission loading limitations and the network congestion conditions have not been considered. Hence, the results obtained are meant as a methodological guide to be used in preliminary power system design only and not for direct implementation in real-time security-constrained system operation.

5.2. Step 2: optimal placement of RES locations as a control variable

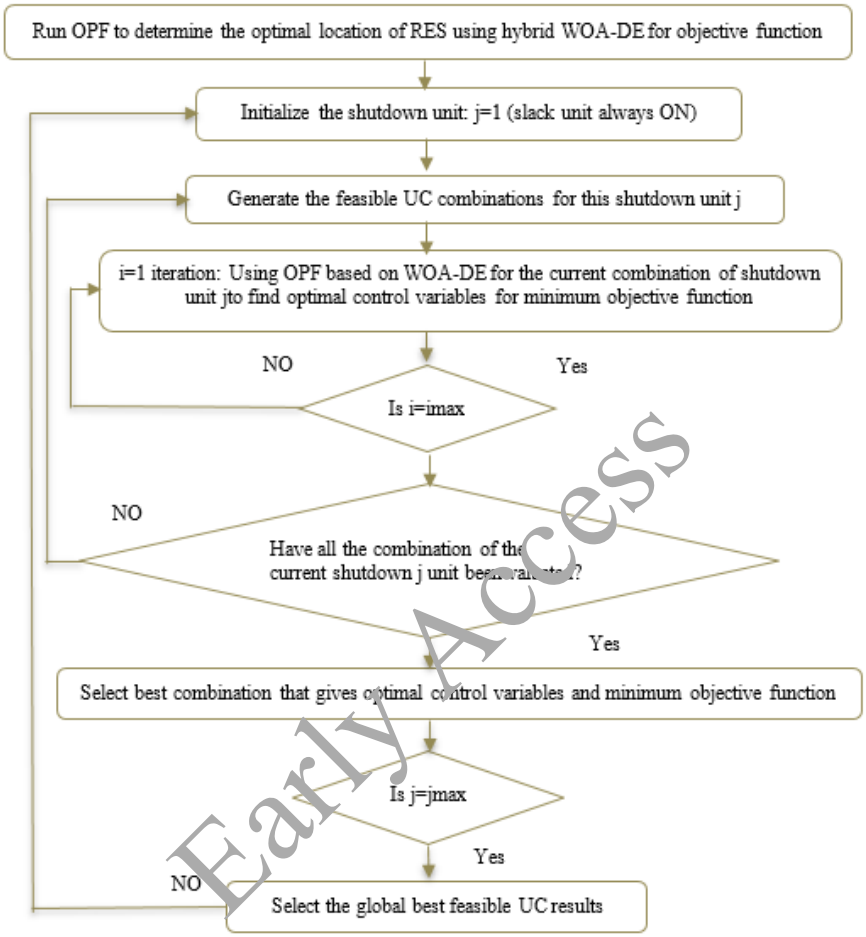
In this step the RES will be added to the system by pre-establishing their sizes and optimizing their locations using OPF based on the WOA-DE [24]. The placement variable will be converted into the solution vector, and the evaluation will be based on the load-flow results obtained by solving the OPF for each configuration. Two different RES placement criteria will be established: the best location based on cost and the best location for the lowest losses.

5.3. Step 3: Unit Commitment with RES based on OPF

In unit commitment with RES sources, for each shutdown for the units, OPF has been used based on the WOA-DE to minimize the fuel cost or losses. UC will decide whether the thermal generation units will be online or offline. The RES units are not part of the thermal-unit switching vector, they will be treated as fixed renewable injections according to the selected renewable model and OPF placement case [25], [26], [27]. The UC objective function adopted in this paper aims to reduce the operating costs of all thermal units that were online after OPF and the RES were integrated, as shown in Fig. 1.

Early Access

This paper has been accepted for publication in the AEE journal. This is the version, which has not been fully edited and content may change prior to final publication.
Citation information: DOI 10.24425/aee.2027.8064



Early Access

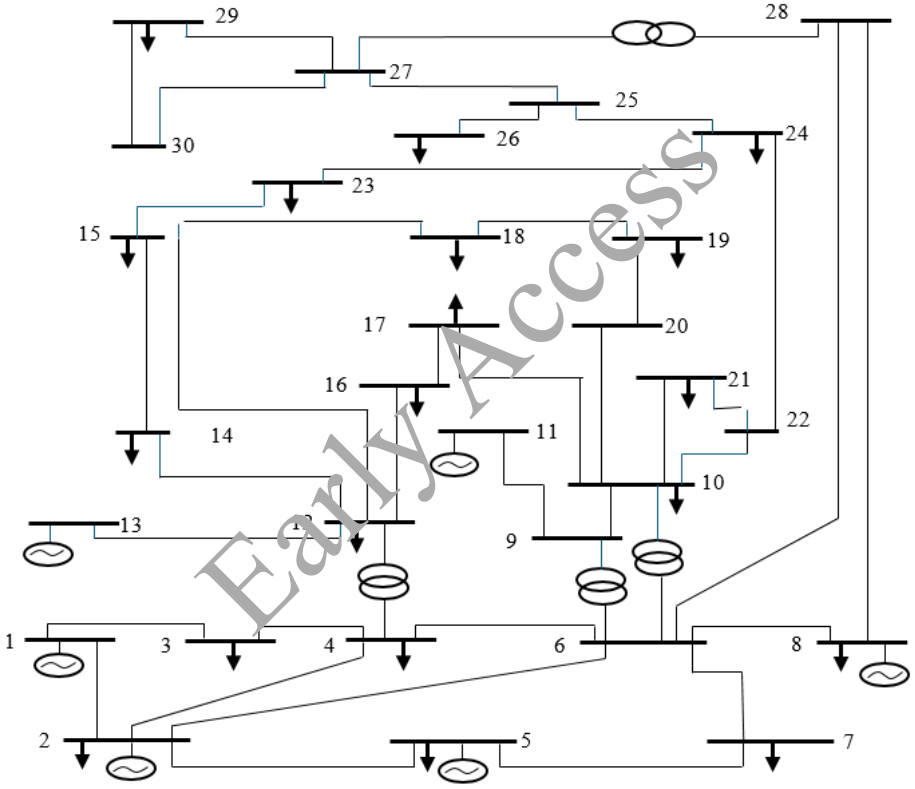
Fig. 1. Proposed RES-UC-OPF methodology

The problem of unit commitment is described as a single-period unit commitment (SP-UC) problem in this research. The operational status of units is determined for one specific power demand, unlike other approaches that employ a multi-hour scheduling method. Thus, the framework discussed here identifies valid combinations of ON/OFF statuses of generating units for a particular operating condition, with generation scheduling done according to optimal power flow analysis.

6. Results and discussion

This paper has been accepted for publication in the AEE journal. This is the version, which has not been fully edited and content may change prior to final publication.
Citation information: DOI 10.24425/aee.2027.8064

The Unit Commitment (UC) of thermal generation units in this article has been improved based on Optimal Power Flow (OPF) and the optimal location of Renewable Energy Sources (RESs). All optimal power-flow calculations and optimization simulations were performed using MATLAB. The Newton–Raphson method was employed for the power-flow calculations. This problem has been tested and solved for the IEEE 30 bus system in Fig. 2. This test system comprises 24 control variables: the active power outputs of five PV bus generators, six generator voltage magnitudes, four transformer taps, and nine shunt reactive power compensators.



Early Access

Fig. 2. Single-line diagram of IEEE 30 bus system

The initial, minimum, and maximum limits of the control variables of the IEEE 30 bus have been presented in Table 2. Also, the OPF problem for the system has been solved based on WOA, DE, and hybrid WOA-DE optimization techniques, where all the optimal control variables for both minimum single-objective approaches of fuel cost and active power losses have been presented separately for each one, satisfying all the state variables of slack active power, load voltage, and generators reactive power in their limits.

This paper has been accepted for publication in the AEE journal. This is the version, which has not been fully edited and content may change prior to final publication.
Citation information: DOI 10.24425/aee.2027.8064

According to Table 2, the hybrid WOA-DE gives better results than WOA and DE optimization techniques.

Table 2. Base optimal power load flow results of the IEEE 30 bus system

Control variables		Limits		Initial value	Optimal control value when the objective is					
		Min	max		Fuel cost ($/h)			Losses (MW)		
					WOA	DE	WOA-DE	WOA	DE	WOA-DE
Generators output (MW)	P2	20	80	80	48.441	48.845	48.7023	80	79.973	80
	P5	15	50	50	21.39	21.265	21.308	50	50	50
	P8	10	35	20	21.02	21.154	21.102	35	35	35
	P11	10	30	20	11.926	11.863	11.892	30	29.995	30
	P13	12	40	20	12	12.004	12	40	39.997	40
Generators voltage (p.u.)	V 1	0.95	1.1	1.05	1.1	1.1	1.1	1.0878	1.099	1.1
	V 2	0.95	1.1	1.04	1.087	1.088	1.0878	1.0833	1.096	1.097
	V 5	0.95	1.1	1.01	1.060	1.062	1.0614	1.0636	1.078	1.079
	V 8	0.95	1.1	1.01	1.099	1.071	1.0693	1.1	1.0863	1.086
	V 11	0.95	1.1	1.05	1.1	1.098	1.1	1.1	1.09	1.1
	V 13	0.95	1.1	1.05	1.1	1.098	1.1	1.1	1.099	1.1
Tap position	T 4-12	0.9	1.1	1.032	1.012	1.018	1.0091	0.97508	0.999	0.996
	T 6-9	0.9	1.1	1.078	0.971	1.066	1.0736	1.0092	1.064	1.074
	T 6-110	0.9	1.1	1.069	0.982	0.905	0.9	0.9	0.906	0.9
	T28-27	0.9	1.1	1.068	0.981	0.983	0.97411	0.95213	0.977	0.978
Injection reactive power compensative device (MVAr)	QC10	0	5	0	1.604	4.785	5	5	4.971	5
	QC12	0	5	0	4.784	4.348	5	5	5	5
	QC15	0	5	0	0	3.710	5	5	4.554	5
	QC17	0	5	0	4.850	4.999	5	5	4.939	5
	QC20	0	5	0	4.987	4.856	5	5	4.884	5

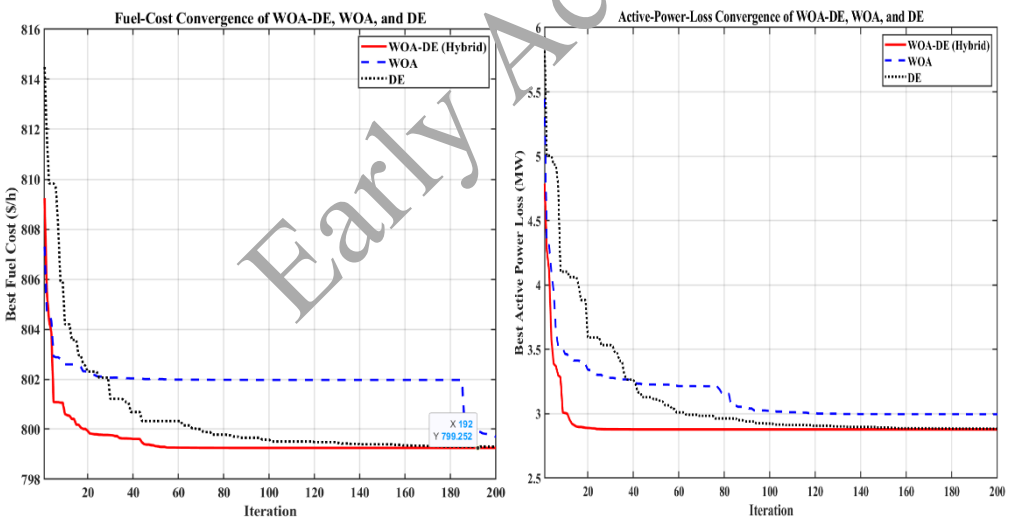
Early Access

This paper has been accepted for publication in the AEE journal. This is the version, which has not been fully edited and content may change prior to final publication.
Citation information: DOI 10.24425/aee.2027.8064

	QC21	0	5	0	0	5	5	5	5	5
	QC23	0	5	0	0	4.165	3.957	1.745	5	4.090
	QC24	0	5	0	5	4.725	5	5	4.956	5
	QC29	0	5	0	3.004	3.9539	3.057	1.042	2.682	2.931
Fuel cost ($/h)				902.058	799.708	799.291	799.251	967.463	967.195	967.181
Losses (MW)				5.841	8.798	8.664	8.656	2.882	2.996	2.878

The curves in Fig. 3 illustrate the comparison of the speed of convergence of the WOA, DE algorithm, and a hybrid WOA-DE algorithm for a single run in terms of minimization of fuel cost and the active power losses. The hybrid WOA-DE algorithm performance is better than the other two optimization techniques. The reason behind the superior performance of the hybrid algorithm is its compatibility of global exploration of WOA and good local exploitation of DE, which leads to enhancing the quality of obtained solutions and speed of convergence. The results were assessed for their effects on the systems technical and economic performance.

Early Access



(a) (b)

Fig. 3. IEEE 30 bus optimal power flow based on: (a) min fuel cost; (b) min active power loss

The statistical comparison of the WOA and DE, as well as the proposed WOA-DE, is provided in Table 3 for 30 independent runs.

Table 3. Statistical results based on 30 independent runs for the minimum objective function

Objective function	Algorithm	Best	Mean	Worst	Std	Time (s)

This paper has been accepted for publication in the AEE journal. This is the version, which has not been fully edited and content may change prior to final publication.
Citation information: DOI 10.24425/aee.2027.8064

Fule cost $/h	**WOA**	799.263	799.525	799.822	0.149	19.527
	DE	799.258	799.269	799.292	0.009	12.755
	WOA-DE	799.252	799.253	799.284	0.005	30.687
Active power losses (MW)	**WOA**	2.879	2.947	3.396	0.111	13.508
	DE	2.879	2.880	2.885	0.001	9.206
	WOA-DE	2.878	2.878	2.890	0.002	33.374

For fuel cost minimization, the WOA-DE shows the best performance in terms of the best cost, the mean cost, and the worst cost while also having the lowest standard deviation, indicating high quality of the solutions. For the minimization of active power loss, the WOA-DE presents the minimum of the best value of the active power loss as well as the minimum value of the mean active power loss, while DE shows the best deviation. With regard to computational time, the WOA-DE shows the longest average computational time since the hybrid method involves additional searches based on WOA and DE.

Table 4 shows a comparison between the proposed algorithm of the WOA-DE and other optimization techniques according to minimum fuel cost. According to this comparison, it is shown that the proposed hybrid WOA-DE method gives the minimum cost of operation as 799.251 $/h, which is less than that obtained from other comparison methods, such as Enhanced Equilibrium Optimizer (EEO) [28], Jaya Algorithm (JAYA) [29], and Improved Cross Entropy Method Assisted with a Chaotic Operator (CGSCE) [30]. It can also be seen that the active power losses obtained with the WOA-DE method are much lower than those of other methods at 8.656 MW. Overall, the results consistently demonstrate the superior performance of the WOA-DE.

Early Access

Table 4. Results of minimum fuel cost based on WOA-DE as compared with other algorithms for the IEEE 30 bus system

Algorithm	**Fuel cost ($/h)**	**Losses (MW)**
EEO [28]	800.4145	8.99217
JAYA [29]	800.4794	9.06481
CGSCE [30]	800.5106	9.02776
WOA-DE/proposed	799.251	8.656

The analysis covers optimal power flow, optimal placement of the RES, and unit commitment. In these cases, the control variables are optimally adjusted to minimize both fuel costs and active power losses while maintaining the system's operational constraints. Finally, the results of both systems are compared and analyzed.

This paper has been accepted for publication in the AEE journal. This is the version, which has not been fully edited and content may change prior to final publication.
Citation information: DOI 10.24425/aee.2027.8064

Based on these optimized OPF values, a sequential unit commitment process was carried out to determine whether some generating units could be de-committed while ensuring the continued feasibility of AC power flow, as shown in Table 4 for a total load demand of 283.42 MW. If the power generation should shut down, the units will not be able to supply the load demand; this case of unit commitment will be infeasible. In order to keep it simple, the total number of unit commitment combinations is provided only for the minimum-cost scenario before the integration of renewable energy sources, while the optimal commitment configuration is provided for all other scenarios and objectives. However, it should be clear that every possible scenario was separately optimized.

The results of the WOA-DE from Table 2 (all units are on) and Table 5 (in case all units are on 111111) showed the relationship between OPF-based control variables and the scheduling of generation units, total fuel cost, total power losses, and system generation feasibility. Therefore, for each scheduling of generation units, there is an optimization for the total control variables based on the WOA-DE.

Table 5. Unit commitment improvement based on OPF for minimum fuel cost for IEEE 30 bus without RES (PD = 283.42 MW).

No	K_{Off}	UC	P1	P2	P5	Po	P11	P13	P losses (MW)	Fuel cost ($/h)
1	0	111111	177.07	48.70	21.30	21.10	11.89	12	8.66	799.25
2	1	101111	200	0	23.65	35	17.18	16.33	8.75	847.18
3	1	110111	188.33	51.54	0	27.06	13.94	13.04	10.50	830.48
4	1	111011	190.75	52.12	22.35	0	14.70	13.72	10.14	805.33
5	1	111101	183.46	50.25	21.79	24.92	0	12.21	9.23	803.32
6	1	111110	183.06	50.14	21.75	24.52	12.99	0	9.07	802.84
7	2	100111	200	0	0	35	29.96	28.66	10.21	892.83
8	2	101011	200	0	30.28	0	30	32.25	9.12	872.90
9	2	101101	200	0	28.81	35	0	28.47	8.87	860.39
10	2	101110	200	0	28.28	35	28.71	0	8.57	858.98
11	2	110011	200	58.18	0	0	19.28	18.10	12.14	840.68
12	2	110101	195.56	53.30	0	31.43	0	14.35	11.23	836.16
13	2	110110	195.09	53.18	0	30.95	15.21	0	11.03	835.53
14	2	111001	200	55.23	23.37	0	0	16.19	11.38	812.69
15	2	111010	200	54.55	23.15	0	16.78	0	11.07	811.59
16	2	111100	Infeasible							
17	3	100011	Infeasible							
18	3	100101	Infeasible							

Early Access

This paper has been accepted for publication in the AEE journal. This is the version, which has not been fully edited and content may change prior to final publication.
Citation information: DOI 10.24425/aee.2027.8064

19	3	100110	Infeasible						
20	3	101001	Infeasible						
21	3	101010	Infeasible						
22	3	101100	Infeasible						
23	3	110001	Infeasible						
24	3	110010	200	68.93	0	0	27.25	0	12.76	854.10
25	3	110100	Infeasible						
26	3	111000	200	68.36	27.28	0	0	0	12.23	825.23
27	4	100001	Infeasible						
28	4	100010	Infeasible						
29	4	100100	Infeasible						
30	4	101000	Infeasible						
31	4	110000	Infeasible						
32	5	100000	Infeasible						

The best shutdown pattern is then selected for each gradual shutdown case based on the shutdown combination that yields the minimum fuel cost and minimum losses, as shown in Tables 6 and 7, respectively.

Early Access

Table 6. Best unit commitment improvement based on OPF for minimum fuel cost for the IEEE 30 bus system without RES (PD = 283.42 MW)

No	K_{Off}	**UC**	**P1**	**P2**	**P5**	**P8**	**P11**	**P13**	***P* losses (MW)**	**Cost ($/h)**
1	0	111111	177.37	48.70	21.30	21.10	11.89	12	8.656	799.25
2	1	111110	183.06	50.14	21.75	24.52	12.99	0	9.069	802.84
3	2	111010	200	54.52	23.15	0	16.78	0	11.069	811.59
4	3	111000	200	68.36	27.28	0	0	0	12.228	825.23
5	4	Infeasible								
6	5	Infeasible								

Table 7. Best unit commitment improvement based on OPF for minimum losses for the IEEE 30 bus system without RES (PD = 283.42 MW)

No	K_{Off}	**UC**	**P1**	**P2**	**P5**	**P8**	**P11**	**P13**	***P* losses (MW)**	**Cost ($/h)**
1	0	111111	80	50	35	30	40	80	2.878	967.182
2	1	111101	80	50	35	30	0	80	4.185	933.014

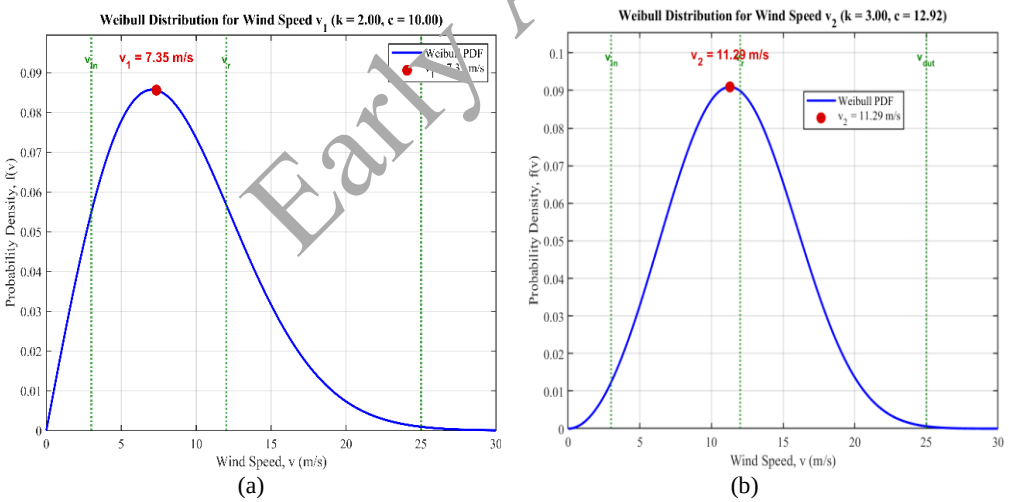
This paper has been accepted for publication in the AEE journal. This is the version, which has not been fully edited and content may change prior to final publication.
Citation information: DOI 10.24425/aee.2027.8064

3	2	111100	80	50	35	30	0	0	6.347	888.885
4	3	110010	80	50	0	0	40	0	12.054	864.450
5	4	Infeasible								
6	5	Infeasible								

Renewable energy resource integration is completed in the second stage; the two wind farm configurations presented are adopted, and the rated capacity of each wind farm is assumed to be 10 MW. The fluctuations in wind speeds were described by means of Weibull distribution. For both wind farms, the turbine power curve was defined and set up using a cut-in wind speed of v_{in} = 3 m/s, a rated wind speed of v_r = 2 m/s, and cut-out wind speeds of v_{out} = 5 m/s. Wind speed of 7.35 m/s with parameter values k = 2 and c = 10 m/s and 11.9 m/s with parameter values k = 3 and c = 12.92 m/s were generated by using the Weibull probability distribution as shown in Fig. 4.

Furthermore, using the wind speed regions in Eq. (10) to find the final output power of wind turbine, where these speeds have been converted to the wind power outputs of 1.1258 MW and 7.8087 MW, respectively. Therefore, together (1.1258 + 7.8087 = 8.9345 MW), these wind power outputs were kept fixed during the further OPF and unit commitment results.

Early Access



(a) (b)

Fig. 4. Weibull distribution for wind speed curve: (a) first wind farm; (b) second wind farm

The location of each wind farm was incorporated into the optimal power flow formulation as an additional control variable. It was selected from a known set of candidate buses, allowing the optimizer, a hybrid Whale Optimization and Differential Evolution (WOA-DE), to determine and select the optimal control variables of the active power of generators except the slack PG; the voltage magnitudes of the generators VG; transformer tap ratios T; shunt compensation QC;

This paper has been accepted for publication in the AEE journal. This is the version, which has not been fully edited and content may change prior to final publication.
Citation information: DOI 10.24425/aee.2027.8064

and the optimal locations of renewable sources, the locations of wind farms, based on the chosen objective function of the minimum fuel cost and the minimum active power losses separately, as shown in Table 8.

Table 8. OPF results with RES placement for the IEEE 30 bus system based on WOA-DE.

Control variables		**Limits**		**Optimal control value when the objective is**	
		Min	**max**	**Fuel cost ($/h)**	**Losses (MW)**
Generators output (MW)	P2	20	80	47.614	79.966
	P5	15	50	20.642	49.999
	P8	10	35	18.958	34.999
	P11	10	30	10.616	29.999
	P13	12	40	12.054	39.999
Generators voltage (p.u.)	V 1	0.95	1.1	1.1	1.099
	V 2	0.95	1.1	1.089	1.099
	V 5	0.95	1.1	1.063	1.082
	V 8	0.95	1.1	1.07	1.092
	V 11	0.95	1.1	1.1	1.098
	V 13	0.95	1.1	1.1	1.096
Tap position	T 4-12	0.9	1.1	1.052	1.009
	T 6-9	0.9	1.1	0.943	1.049
	T 6-110	0.9	1.1	1.044	1.038
	T28-27	0.9	1.1	0.978	1.005
Injection reactive power compensative device (MVAr)	QC10	0	5	4.187	4.999
	QC12	0	5	0.598	4.998
	QC15	0	5	0.843	4.999
	QC17	0	5	0.605	4.895
	QC20	0	5	4.095	4.997
	QC21	0	5	4.784	4.926
	QC23	0	5	3.685	4.367
	QC24	0	5	2.407	4.758

Early Access

This paper has been accepted for publication in the AEE journal. This is the version, which has not been fully edited and content may change prior to final publication.
Citation information: DOI 10.24425/aee.2027.8064

	QC29	0	5	0.491	4.925
Optimal location	WT1 of 1.1258 MW			11 bus	13 bus
	WT2 of 7.8087 MW			5 bus	11 bus
Fuel cost ($/h)				767.135	945.599
Losses (MW)				8.335	2.664

The best shutdown units of unit commitment according to minimum fuel cost and minimum active power losses with the RES are shown in Tables 9 and 10.

Table 9. Best unit commitment improvement based on OPF with RES for minimum fuel cost for the IEEE 30 bus system (PD = 274.49 MW)

No	K_{Off}	UC 5	P1	P2	P5	P8	P11	P13	*P* losses (MW)	Cost ($/h)
1	0	111111	173.835	47.615	20.642	18.058	10.616	12.054	8.335	767.135
2	1	111110	178.470	49.070	21.339	22.096	12.255	0	8.744	770.594
3	2	111100	184.070	51.305	21.643	26.664	0	0	9.197	774.551
4	3	111000	199.980	60.891	25.812	0	0	0	12.198	788.829
5	4	Infeasible								
6	5	Infeasible								

Table 10. Best unit commitment improvement based on OPF with RES for minimum losses for the IEEE 30 bus system (PD = 274.49 MW)

No	K_{Off}	UC	P1	P2	P5	P8	P11	P13	*P* losses (MW)	Cost ($/h)
1	0	111111	42.184	79.966	49.999	34.999	29.999	40	2.664	945.599
2	1	111101	73.317	79.992	49.997	34.997	0	39.980	3.787	908.894
3	2	111100	114.855	79.924	49.984	34.995	0	0	5.365	861.372
4	3	101100	197.600	0	49.999	35,000	0	0	8.114	871.836
5	4	Infeasible								
6	5	Infeasible								

The objectives of the minimum fuel cost and the minimum active power losses of UC without using the RES in Tables 5 and 6, respectively, are compared with the result of Tables 8 and 9 that use the RES. The integration of Renewable Energy Sources (RESs) proves advantageous for system performance at all values of k, in the case of $k = 0$, where all the generating sources are used. In the case of the minimum cost objective, in order to quantify the effect of integrating

Early Access

This paper has been accepted for publication in the AEE journal. This is the version, which has not been fully edited and content may change prior to final publication.
Citation information: DOI 10.24425/aee.2027.8064

Renewable Energy Sources (RESs) on the financial and technical aspects of the system, the decrease in fuel price and active power losses was calculated. The formula for calculating the decrease in fuel price is the following:

$$\Delta\text{Cost} = \frac{\text{C}_{\text{base}} - \text{C}_{\text{RES}}}{\text{C}_{\text{base}}} \times 100\,. \tag{18}$$

C_{base} is the cost of fuel prior to the RES integration, while C_{RES} refers to the fuel price after the RES integration. The calculations have shown that

$$\Delta\text{Cost} = \frac{799.252 - 767.135}{799.252} \times 100 = 4.02\%.$$

The percentage power loss reduction can be calculated according to the following formula:

$$\Delta P_{\text{loss}} = \frac{P_{\text{base}} - p_{\text{RES}}}{p_{\text{base}}} \times 100, \tag{19}$$

where P_{base} and p_{RES} show the active power losses before and after the integration of the RES, respectively. The calculations have shown that

$$\Delta P_{\text{loss}} = \frac{2.878 - 2.664}{2.878} \times 100 = 7.44\%.$$

Thus, the RES integration leads to a reduction of fuel costs in the amount of 32.117 \$/h, which is equal to approximately 4.02%, while the active power loss reduction accounts for 0.214 MW, or around 7.44%. The calculations demonstrate the positive influence of the RES integration on the financial and technical characteristics of the studied power system.

Overall, the results showed that the effective siting of the RES improves the efficiency of the system and reduces the dependence on thermal power generation, thereby lowering power generation and the objective function according to fuel consumption costs or active power losses for the same load demand. This indicates that the proposed OPF-based approach to RES placement could enhance the operational and economic performance of the power system while maintaining a feasible unit commitment schedule.

Early Access

7. Conclusion

This article presented an integrated unit commitment – OPF framework for the IEEE 30 bus system. The first stage included an OPF problem solved with two objectives of minimization fuel cost and active power loss. The results provide the optimal control variables, including generator voltage magnitude, transformer tap setting, reactive power compensation, and active power output of PV generators. Based on optimal control variables, a gradual shutdown procedure for units was implemented. At each shutdown level, the possible combinations were assessed, and the combination with the minimum operating cost and loss that still maintained feasibility for AC power flow was selected.

This paper has been accepted for publication in the AEE journal. This is the version, which has not been fully edited and content may change prior to final publication.
Citation information: DOI 10.24425/aee.2027.8064

Two wind farms have been selected for the IEEE 30 bus system to increase the amount of renewable energy affecting the entire power system. The locations of the renewable resources added to the system were treated as controllable resources in the analysis, and they were optimally located using the optimal power flow methodology. The renewable resources reduced the overall thermal power generation, total operating costs, and active power losses. Relative to the base-case scenario, the unit commitment results indicate that even after integrating renewable resources, the recommended shutdown patterns remain valid and that there are clear economic advantages to their incorporation. Optimal unit commitment analysis based on integrating OPF with optimal siting of the RES enables a more comprehensive approach to enhancing a power systems performance both technically and economically.

When compared to related works that utilize single optimization techniques or solve problems of OPF and UC using various algorithms, the strategy presented in this paper embraces OPF-based unit commitment, renewable energy facilities, and the hybrid WOA-DE methodology in a single optimization framework. The developed approach relies on the strengths of the WOA algorithm in its exploration capability, while the mechanisms of mutation and crossover of DE make it possible to enhance the search process and minimize the risk of early convergence. In practice, the technique introduced here can help operators and owners of power plants in scheduling generation activities and thus reducing costs, as well as achieving the goal of using renewable energy sources without violating system operating requirements. Nonetheless, the current study faces certain restrictions. The proposed technique has been validated just on the testing systems analyzed in this paper, and the computational efficiency of the proposed technique might decrease with increasing size of the power system and longer time horizons. Additionally, the actual OPF model does not include limits over loading the transmission lines or transmission constraints. Thus, the obtained results should be considered merely as preliminary and simplified estimates rather than complete security constrained operational model. Future research will aim at extending the proposed approach to larger power systems, multi-period UC, transmission limits, and energy storage systems.

Early Access

References

[1] Duman S., Li J., Wu L., *AC optimal power flow with thermal–wind–solar–tidal systems using the symbiotic organisms search algorithm*, IET Renewable Power Generation, vol. 15, no. 2, pp. 278–296 (2021), DOI: 10.1049/rpg2.12023.

[2] Alghamdi H., Hua L.-G., Riaz M., Hafeez G., Ullah S., Zaidi M.M., Jalalah M., *An optimal power flow solution for a power system integrated with renewable generation*, AIMS Mathematics, vol. 9, no. 3, pp. 6603–6627 (2024), DOI: 10.3934/math.2024322.

[3] Altai H.D.S., Lpizra A., Saleh A.L., Hazim H.T., Lazim M.H., *Solving Unit Commitment Including Wind Power Generation Using PSS®E*, Misan Journal of Engineering Sciences, vol. 1, no. 1, pp. 69–93 (2022), DOI: 10.61263/mjes.v1i1.25.

[4] Siregar R.H., Akhyar A., Lubis R.S., Hadi M.N., *Optimal Power Flow-Assisted Unit Commitment with Multi-Level Load Variation Analysis in Renewable-Based Power Systems*, Energies, vol. 18, no. 23, 6340 (2025), DOI: 10.3390/en18236340.

This paper has been accepted for publication in the AEE journal. This is the version, which has not been fully edited and content may change prior to final publication.
Citation information: DOI 10.24425/aee.2027.8064

[5] Riaz M., Hanif A., Masood H., Khan M.A., Afaq K., Kang B.-G., Nam Y., *An Optimal Power Flow Solution of a System Integrated with Renewable Sources Using a Hybrid Optimizer*, Sustainability, vol. 13, no. 23, 13382 (2021), DOI: 10.3390/su132313382.
[6] Li Z., Yin H., Wang P., Gu C., Wang K., Hu Y., *A fast linearized AC power flow-constrained robust unit commitment approach with customized redundant constraint identification method*, Frontiers in Energy Research, vol. 11, no. 1218461 (2023), DOI: 10.3389/fenrg.2023.1218461.
[7] Mena R., Godoy M., Catalán C., Viveros P., Zio E., *Multi-objective two-stage stochastic unit commitment model for wind-integrated power systems: A compromise programming approach*, International Journal of Electrical Power & Energy Systems, vol. 152, no. 109214 (2023), DOI: 10.1016/j.ijepes.2023.109214.
[8] Trojani A.G., Moghaddam M.S., Baigi J.M., *Stochastic Security-constrained Unit Commitment Considering Electric Vehicles, Energy Storage Systems, and Flexible Loads with Renewable Energy Resources*, Journal of Modern Power Systems and Clean Energy, vol. 11, no. 5, pp. 1405–1414 (2023), DOI: 10.35833/MPCE.2022.000781.
[9] Niu Q., Tang L., Yu L., Wang H., Yang Z., *Unit Commitment Considering Electric Vehicles and Renewable Energy Integration—A CMAES Approach*, *Sustainability*, vol. 16, no. 3, 1019 (2024), DOI: 10.3390/su16031019.
[10] Al-Bahrani L., Al-Kaabi M., Al-Saadi M., Dumbrava V., *Optimal power flow based on differential evolution optimization technique*, *UPB Scientific Bulletin*, Series C: Electrical Engineering and Computer Science, vol. 82, no. 1, pp. 247–258 (2020).
[11] Al-Kaabi M., Al Hasheme J., Al-Bahrani L., *Improved Differential Evolution Algorithm to solve multi-objective of optimal power flow problem*, Archives of Electrical Engineering, vol. 71, no. 3, pp. 641–657 (2022), DOI: 10.24425/aee.2022.141676.
[12] Nassef A.M., Abdelkareem M.A., Louzazni M., *Optimal power flow using recent red-tailed hawk optimization algorithm*, Results in Engineering, vol. 25, no. 104005 (2025), DOI: 10.1016/j.rineng.2025.104005.
[13] Almansury A.M., Al-Anbarri K.A., *Security Constrained Optimal Power Flow Based on an Artificial Intelligence Technique*, Journal of Engineering and Sustainable Development, vol. 27, no. 6, pp. 725–741 (2023), DOI: 10.31272/jeasd.27.6.5.
[14] Ranarison O.M., Randriamora E., Andriatsihoarana H., *Optimal power flow using Modified Driving-Training Based Optimization algorithm*, International Journal of Advances in Engineering and Management, vol. 7, no. 2, pp. 846–860 (2025), DOI: 10.35629/5252-0702846860.
[15] Adeyemo A.A., Marra F., Tedeschi E., *Sizing of energy storage for spinning reserve and efficiency increase in isolated power systems within a data-driven stochastic unit commitment framework*, Journal of Energy Storage, vol. 111, no. 115051 (2025), DOI: 10.1016/j.est.2024.115051.
[16] Mohamed M.I., Ali A.F.M., Yousef A.M., Hafez A.A., *Autonomous dynamic economic dispatch with limited fuel and renewable energy sources using marine predators optimizer*, Scientific Reports, vol. 16, no. 13518 (2026), DOI: 10.1038/s41598-026-48247-2.
[17] Wang Z., Wang X., Liu W., *Genetic least square estimation approach to wind power curve modelling and wind power prediction*, Scientific Reports, vol. 13, no. 9188 (2023), DOI: 10.1038/s41598-023-36458-w.
[18] Deshmukh M.K., Deshmukh S.S., *Modeling of hybrid renewable energy systems*, Renewable and Sustainable Energy Reviews, vol. 12, no. 1, pp. 235–249 (2008), DOI: 10.1016/j.rser.2006.07.011.

Early Access

This paper has been accepted for publication in the AEE journal. This is the version, which has not been fully edited and content may change prior to final publication.
Citation information: DOI 10.24425/aee.2027.8064

[19] Pan X., Liu Z., Liu W., Li Y., *Wind farm polymerization influences on security and economic operation in power system based on Copula function*, Journal of Modern Power Systems and Clean Energy, vol. 3, no. 3, pp. 381–392 (2015), DOI: 10.1007/s40565-015-0147-6.

[20] Tang R., Tang X., Zhao H., *Enhancing Whale Optimization Algorithm with Differential Evolution and Lévy Flight for Robot Path Planning*, International Journal of Advanced Computer Science and Applications, vol. 15, no. 5, pp. 401–410 (2024), DOI: 10.14569/IJACSA.2024.0150540.

[21] Xi J., Chen Y., Liu X., Chen X., *Whale Optimization Algorithm based on Nonlinear Adjustment and Random Walk Strategy*, Journal of Network Intelligence, vol. 7, no. 2, pp. 306–318 (2022).

[22] Luo J., Shi B., *A hybrid whale optimization algorithm based on modified differential evolution for global optimization problems*, Applied Intelligence, vol. 49, no. 5, pp. 1982−2000 (2019), DOI: 10.1007/s10489-018-1362-4.

[23] Fadhil M., Al-Bahrani L., *Constrained-Optimal Power Flow with Wind Turbine and Thyristor-Controlled Series Compensator Using DEPSO Algorithm*, International Journal of Intelligent Engineering and Systems, vol. 17, no. 6, pp. 179–193 (2024), DOI: 10.22266/ijies2024.1231.15.

[24] Zaman K., Zhaoyun S., Shah B., Hussain A., Hussain T., Khan U.S., Ali F., Sarra B., *Efficient power management optimization based on whale optimization algorithm and enhanced differential evolution*, Alexandria Engineering Journal, vol. 79, pp. 652–670 (2023), DOI: 10.1016/j.aej.2023.08.045.

[25] Abaci K., Yetgin Z., Yamacli V., Isiker H., *Modified effective butterfly optimizer for solving optimal power flow problem*, Heliyon, vol. 10, no. 12, e32862 (2024), DOI: 10.1016/j.heliyon.2024.e32862.

[26] Lu K.-H., Qian W., Jiang Y., Zhong Y.-S., *The Calibrated Safety Constraints Optimal Power Flow for the Operation of Wind-Integrated Power Systems*, Processes, vol. 12, no. 10, 2272 (2024), DOI: 10.3390/pr12102272.

[27] Ghasemi M., Trojovský P., Trojovská E., Zare M., *Gaussian bare-bones Levy circulatory system-based optimization for power flow in the presence of renewable units*, *Engineering Science and Technology*, an International Journal, vol. 47, no. 101551 (2023), DOI: 10.1016/j.jestch.2023.101551.

[28] Houssein E.H., Hassan M.H., Mahdy M.A., Kamel S., *Development and application of equilibrium optimizer for optimal power flow calculation of power system*, Applied Intelligence, vol. 53, pp. 7232–7253 (2023), DOI: 10.1007/s10489-022-03796-7.

[29] Warid W., Hizam H., Mariun N., Abdul-Wahab N.I., *Optimal Power Flow Using the Jaya Algorithm*, Energies, vol. 9, no. 9, 678 (2016), DOI: 10.3390/en9090678.

[30] Su H., Niu Q., Yang Z., *Optimal Power Flow Using Improved Cross-Entropy Method*, Energies, vol. 16, no. 14, 5466 (2023), DOI: 10.3390/en16145466.

Early Access